Biophysical Reviews (2017) 9:861–876
https://doi.org/10.1007/s12551-017-0335-x

REVIEW

Conversion of microbial rhodopsins: insights into functionally essential elements and rational protein engineering

Akimasa Kaneko[1] · Keiichi Inoue[2,3,4] · Keiichi Kojima[5] · Hideki Kandori[2,3] · Yuki Sudo[1,5]

Received: 12 August 2017 / Accepted: 7 November 2017 / Published online: 25 November 2017

Abstract

Technological progress has enabled the successful application of functional conversion to a variety of biological molecules, such as nucleotides and proteins. Such studies have revealed the functionally essential elements of these engineered molecules, which are difficult to characterize at the level of an individual molecule. The functional conversion of biological molecules has also provided a strategy for their rational and atomistic design. The engineered molecules can be used in studies to improve our understanding of their biological functions and to develop protein-based tools. In this review, we introduce the functional conversion of membrane-embedded photoreceptive retinylidene proteins (also called rhodopsins) and discuss these proteins mainly on the basis of results obtained from our own studies. This information provides insights into the molecular mechanism of light-induced protein functions and their use in optogenetics, a technology which involves the use of light to control biological activities.

Keywords Rhodopsin · Energy conversion · Signal transduction · Membrane protein · Retinal

Introduction

Recent progress in molecular and structural biological techniques has achieved many functional insights into biomolecules, such as nucleotides and proteins. Such information has allowed the modification, conversion and production of molecules in extensive experimental and theoretical studies (Huang et al. 2016). One example of this progress is a membrane-embedded photoactive protein, rhodopsin, which is a member of the seven-transmembrane (TM) domain protein family that uses a retinal pigment (a derivative of vitamin A) as a chromophore. This chromophore is covalently attached to the apoprotein opsin via a protonated Schiff base linkage with a perfectly conserved Lys residue, as shown in Fig. 1a (Spudich and Jung 2005; Ernst et al. 2014). Since 2000, genomic analyses have revealed a large variety of rhodopsin molecules in nature, and those rhodopsins, including newly discovered ones, are categorized into two types, namely animal and microbial rhodopsins (Ernst et al. 2014). Microbial rhodopsins, also called type-1 rhodopsins, are widely distributed among the microbial kingdom, including the bacteria, archaea and eukarya, as shown in Fig. 1b, and they work as light-dependent ion transporters and photosensors (Hegemann 2008; Ernst et al. 2014; Kurihara and Sudo 2015; Schneider et al. 2015; Brown and Ernst 2017; Govorunova et al. 2017). Animal rhodopsins, also called type-2 rhodopsins, are mainly distributed in both vertebrates and invertebrates, and they typically work as visual photoreceptors in cellular membranes to capture light signals and transfer them to their cytoplasmic cognate G-proteins in the retina (Shichida and Imai 1998). In general, light absorption of type-1 and type-2 rhodopsins triggers *trans–cis* and *cis–trans* isomerization of the retinal chromophore, respectively, leading to structural changes of the protein moiety during the photoreaction for their cognate biological functions (Ernst et al. 2014). The reaction for type-1 rhodopsins is a cyclic one called the photocycle (Lanyi 2004), while that for type-2 rhodopsins is unidirectional or bidirectional (Shichida and Imai 1998; Koyanagi and Terakita 2008).

✉ Yuki Sudo
sudo@okayama-u.ac.jp

[1] Faculty of Pharmaceutical Sciences, Okayama University, Okayama 700-8530, Japan

[2] Department of Frontier Materials, Nagoya Institute of Technology, Showa-ku, Nagoya 466-8555, Japan

[3] OptoBioTechnology Research Center, Nagoya Institute of Technology, Showa-ku, Nagoya 466-8555, Japan

[4] Precursory Research for Embryonic Science and Technology (PRESTO), Japan Science and Technology Agency (JST), 4-1-8 Honcho Kawaguchi, Saitama 332-0012, Japan

[5] Graduate School of Medicine, Dentistry and Pharmaceutical Sciences, Okayama University, 1-1-1 Tsushima-naka, Kita-ku, Okayama 700-8530, Japan

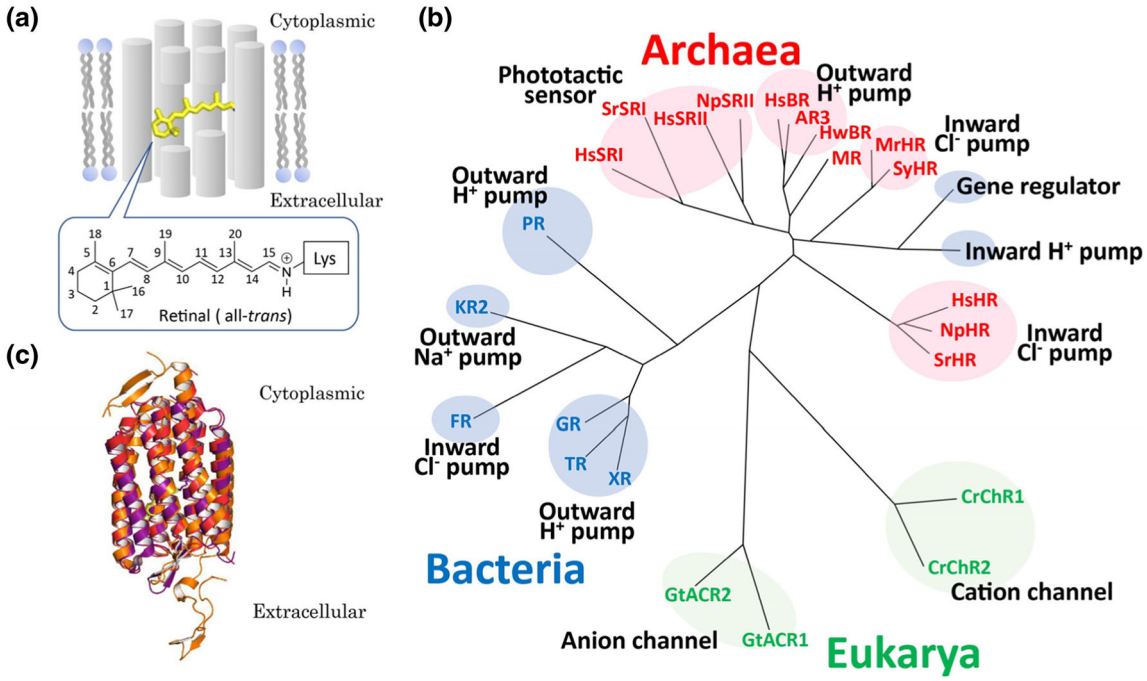

Fig. 1 Overview of microbial rhodopsins. **a** Schematic drawing of a seven-transmembrane microbial rhodopsin, where an all-*trans* retinyl chromophore (yellow) is covalently tethered to a specific Lys residue of the apoprotein opsin via a protonated Schiff base linkage. Numbers on the retinal represent the cognate carbon atoms. **b** Phylogenetic tree of microbial rhodopsins constructed by ClustalW software program. Microbial rhodopsins are widely distributed throughout all domains of organisms, bacteria (blue), eukarya (green) and archaea (red), with a wide variety of biological functions (pumps, channels and sensors). See text for the abbreviations of the names of microbial rhodopsins. **c** Superposition of crystal structures of *Halobacterium salinarum* bacteriorhodopsin (purple) (HsBR; PBD ID 1C3W), *Natronomonus pharaonis* sensory rhodopsin II (red) (NpSRII; PBD ID 1JGJ) and chimeric cation channelrhodopsin (ChR) from *Chlamydomonas reinhardtii* ChR-1 (CrChR1) and ChR-2 (CrChR2) (orange) (C1C2; PDB ID 3UG9). The retinal chromophore is colored yellow

The first microbial type-1 rhodopsin identified, bacteriorhodopsin (BR), was isolated from the archaeon *Halobacterium salinarum* (formerly *halobium*) in 1971 as a light-driven outward H^+ pump, and it was thereafter called *H. salinarum* BR (HsBR). The H^+ pumping function of HsBR results in the light-dependent generation of an H^+ gradient [proton motive force (PMF)] between the inside and the outside of the plasma membrane (Oesterhelt and Stoeckenius 1971, 1973). The PMF is used to synthesize ATP (Racker and Stoeckenius 1974). In addition to its biological significance, the high stability and high level of protein expression in native membranes have allowed the extensive analysis of HsBR as a model of both membrane proteins and light-activated molecules (Lanyi 2004). Light absorption by HsBR results in the sequential appearance of several photointermediates during the photocycle, namely K_{590}, L_{550}, M_{410}, N_{560} and O_{640}, followed by a return to the initial form (Lanyi 2004). The numbers denote wavelengths (in nm) of the maximum absorption (λ_{max}) in the visible region. After the discovery of HsBR, functionally different types of microbial type-1 rhodopsins were successively identified in various species: an inward chloride (Cl^-) pump (Matsuno-Yagi and Mukohata 1977; Schobert and Lanyi 1982), an outward sodium (Na^+) pump (Inoue et al. 2013a), an inward proton (H^+) pump (Inoue et al. 2016a), light-gated cation (Nagel et al. 2002; Nagel et al. 2003) and anion channels (Govorunova et al. 2015), phototactic sensors (Bogomolni and Spudich 1982; Takahashi et al. 1985; Inoue et al. 2013b), a light-induced transcriptional regulator (Jung et al. 2003; Irieda et al. 2012) and light-dependent enzymes (Luck et al. 2012; Avelar et al. 2014) (Fig. 1b). In spite of both the rich functional differentiation and the variety of amino acid sequences (identity: 11 - 48%, similarity: 43 - 76%), the X-ray crystal structures determined so far are surprisingly well matched, especially their TM helices (root-mean-square deviation is less than ~ 2 Å), as shown in Fig. 1c. This indicates that their functional differences are regulated by relatively small differences in their side chains, water molecules and ions. To reveal the structural and functional correlations and to identify the key elements determining their functions, we performed and succeeded in the functional conversion of microbial rhodopsins by site-specific replacement of their amino acid residues. In this review, we introduce those studies and explain the insights which have been obtained with the aim to gain an understanding of the mechanism of their biological functions and to utilize them for optogenetics, a technology which involves the use of light to control biological activities (Boyden et al. 2005; Deisseroth 2015).

Conversion of outward proton pumps

Chloride pump

Halobacterium salinarum BR first became a focus of interest as a template for converting it into molecules having different kinds of functions (Fig. 2). In 1995, our colleague J. Sasaki succeeded in converting HsBR into a mutant functioning as a light-driven inward Cl^- pump, with Asp85 of HsBR replaced by Thr or Ser (Fig. 2a) (Sasaki et al. 1995). The critical residue Asp85 is known to be deprotonated in the unphotolyzed state, and it works as a counterion of the protonated Schiff base (Lys216 in HsBR) of the retinal chromophore (Marti et al. 1991). Upon formation of the early photointermediates, the all-*trans* retinal chromophore changes to 13-*cis*, and the stored energy induces sequential protein conformational changes (Ernst et al. 2014). Upon formation of the M-intermediate, the proton of the protonated Schiff base nitrogen is transferred to the nearby deprotonated Asp85 (Braiman et al. 1988). In the natural Cl^- pump halorhodopsin (HR), the aspartate is replaced by a Thr residue [Thr111 for *H. salinarum* HR (HsHR)] and, consequently, the photocycle of HRs lacks the M-intermediate (Váró et al. 1995a, b; Váró 2000). Thus, the functional conversion of HsBR into an HsHR-like Cl^- pump revealed that Asp85 is not only a proton acceptor, but also a determinant of ion selectivity. This also revealed that the essential features of the H^+ transport mechanism of HsBR are commonly conserved in the anion transport mechanism in the inward Cl^- pump HsHR, in spite of the amino acid sequence differences between HsBR and HsHR (identity = 30%, similarity = 68%).

Proton channel

Ion pumps such as HsBR and HsHR actively transport ions against the concentration gradient, while ion channels

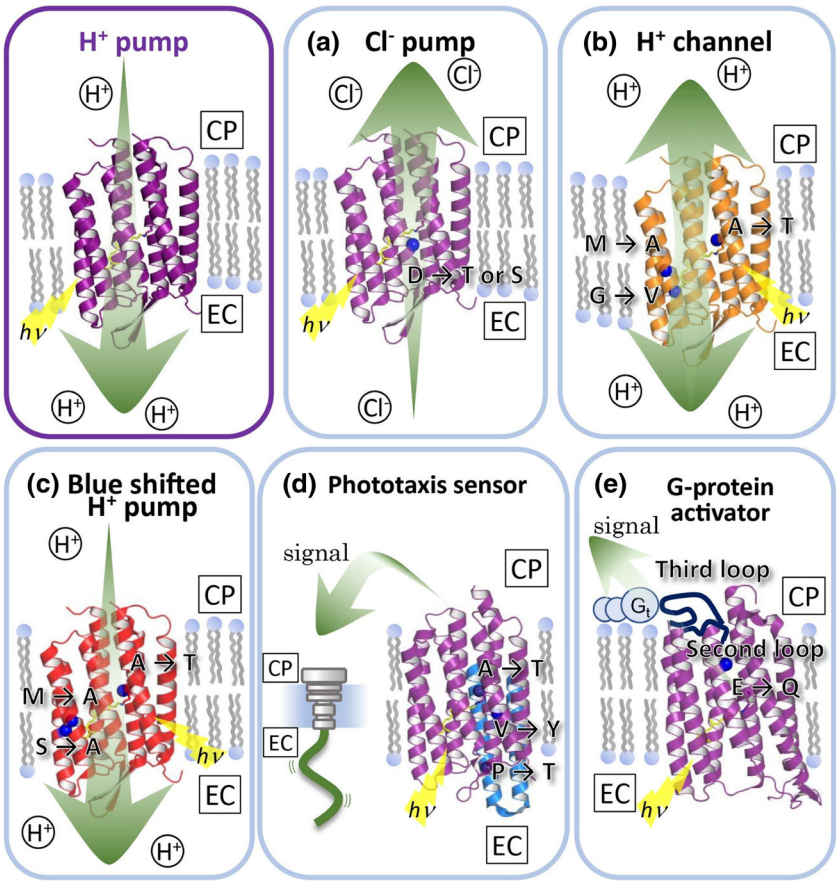

Fig. 2 Conversion of outward proton pumps with respect to the light-driven outward proton (H^+) pumping rhodopsin HsBR and its homologous proteins archaerhodopsin-3 (AR3), *Haloquadratum walsbyi* bacteriorhodopsin (HwBR) and *Gloeobacter* rhodopsin (GR). **a**–**d** Structures from HsBR (PBD ID 1C3W) (**a**–**c**) and from the complex of NpSRII (purple) and halobacterial transducer protein II (HtrII; blue) (PBD ID 1H2S) (**d**).**e** Structure from thermophilic rhodopsin (TR; PBD ID 5AZD). **a** Conversion of HsBR into a light-driven inward chloride (Cl^-) pump by a single amino acid substitution (D85T or D85S). **b** Conversion of AR3 into a light-gated H^+ channel by three amino acid substitutions (M126A/G130 V/A225T). **c** Conversion of HwBR and AR3 into a blue-shifted H^+ pump by three amino acid substitutions (triple mutants; M126A/S149A/A223T for HwBR and M128A/S151A/A225T for AR3). **d** Conversion of HsBR into a negative phototaxis sensor by three amino acid substitutions (P200T/V210Y/A215T). **e** Conversion of GR into a light-dependent G-protein activator by substitutions of the second and third cytoplasmic loops and a residue (E132Q). The word "*hν*" stands for the light energy. CP Cytoplamic sites, EC extracellular sides

passively transport ions upon stimulation corresponding to the concentration gradient (Grote et al. 2014). After 2002, research on a novel microbial rhodopsin named channelrhodopsin (ChR) revealed its wide distribution in eukaryotic algae and that it functions as a light-gated cation channel (Hou et al. 2012). The first ChRs reported were *Chlamydomonas reinhardtii* ChR-1 (CrChR1) and ChR-2 (CrChR2) (Fig. 1b), which nonspecifically transport several types of cations (H^+, Na^+, K^+ and Ca^{2+}) (Nagel et al. 2002, 2003). Since then, homologous ChRs have been reported for various species of algae, such as *Volvox carteri* (VChR1 and VChR2), *Chlamydomonas augustae* (CaChR1) and *Mesostigma viride* (MvChR1) (Ernst et al. 2008; Govorunova et al. 2011; Hou et al. 2012; Ogren et al. 2014). The X-ray crystallographic structure of a chimeric ChR between CrChR1 and CrChR2 (named C1C2) was solved in 2012 by the Nureki group (Kato et al. 2012). To investigate essential differences between pumps and channels, in 2015 we tried to convert an HsBR-like archaeal H^+ pump, archaerhodopsin-3 (AR3; see Fig. 1b), into a ChR-like light-gated H^+ channel (Fig. 2b) (Inoue et al. 2015). In that study, comparison of the structures of C1C2 and HsBR (Luecke et al. 1999) revealed that the β-ionone ring of the retinal in C1C2 moves slightly to the cytoplasmic side compared to HsBR. We hypothesized that this structural difference in the retinal chromophore is responsible for the functional differentiation. Based on a comparison of the amino acid sequences between pumps and channels, we focused on three residues and mutated them in AR3 (Fig. 2b). Two of these, M126A and G130 V, changed the structure of the β-ionone ring by the removal of steric hindrance in AR3, while the other one, A225T, controlled the hydrophilicity around the Schiff base. As a result, we succeeded in the functional conversion of AR3 into an H^+ channel by three substitutions (Inoue et al. 2015). A similar strategy for the functional conversion of AR3 could be successfully applied to another representative archaeal H^+ pump, *Haloquadratum walsbyi* BR (HwBR), but not to a eubacterial H^+ pump [*Gloeobacter violaceus* rhodopsin (GR)], indicating that functional conversion is evoked only for archaeal H^+ pumps (AR3 and HwBR) and not for the eubacterial pump GR (Fig. 1b) (Inoue et al. 2015). Thus, these successful functional conversions revealed the relationship between pumping and channeling rhodopsins, in spite of their amino acid sequence differences (e.g. identity = 22% and similarity = 67% between AR3 and C1C2).

Color variant

One of the characteristics of animal and microbial rhodopsins is the wide variety of their absorption maxima (colors), which range from ~ 360 to 620 nm and are regulated by interactions between the apoprotein opsin and the retinyl chromophore (Katayama et al. 2015). The archaeal proton pumping rhodopsins, such as HsBR, HwBR and AR3, show absorption maxima at ~ 560 nm with a purple color (Sudo et al. 2013). Several mechanisms have been proposed for spectral tuning (Katayama et al. 2015). Briefly, three key factors are important: (1) electrostatic interactions between the chromophore and its counterion (deprotonated carboxylates or negatively charged ions such as Cl^-); (2) alterations in the polarity and/or polarizability of the environment of the chromophore-binding cavity, induced by polar and/or non-polar residues in the protein moiety; and (3) isomerization of the 6-S bond (6,7-torsion angle) connecting the polyene chain to the β-ionone ring, which disrupts the π-conjugation system (see Fig. 1a). By combining these effects, we succeeded in the rational control of the absorption maxima (colors) in various microbial rhodopsins, including HwBR and AR3 (Shimono et al. 2001, 2003; Suzuki et al. 2009; Sudo et al. 2011b). However, these studies did not address the biological functions. In 2013, we attempted to produce a blue-shifted H^+ pump without loss of pumping activity by substituting three amino acid residues (M126A/S149A/A223T). Because factors (1) and (2) are related to the Schiff base region of the retinal chromophore and are tightly coupled with the biological functions via *trans-cis* isomerization, mutations around the Schiff base region are expected to negatively affect the H^+ pumping activity. We then focused on factor (3), which involves the β-ionone ring of the retinal chromophore. The triple mutant (M126A/S149A/A223T) ultimately showed an absorption maximum at 454 nm with a robust H^+ pumping activity (Fig. 2c) (Sudo et al. 2013). To investigate the explanation for the large spectral blue shift, we also performed molecular dynamics (MD) simulations. As expected, the isomerization of the β-ionone ring was confirmed in that mutant (Sudo et al. 2013). The large spectral shift caused by the three substitutions (M126A/S149A/A223T) can be successfully applied to other microbial rhodopsins, such as HwBR and C1C2, indicating the universality of our strategy. In addition, the color variants have been successfully utilized in optogenetics as both neural silencers and activators in living cells (Kato et al. 2015b).

Phototaxis sensor

Organisms live in various environments by changing their motility to migrate toward more favorable habitats, termed positive taxis, and to avoid harmful ones, termed negative taxis (Suzuki et al. 2010). Light is one of the most important external signals that provides critical information to biological systems, and therefore organisms utilize light not only as an energy source but also as a signal. Thus, in addition to the ion transporting rhodopsins, there are microbial rhodopsins functioning as light-signal transducers in nature (Fig. 1b). The first photosensory rhodopsin, named sensory rhodopsin I (SRI), was identified in the archaeon *H. salinarum* in 1982 as a dual

photoreceptor for two opposite functions, positive and negative phototaxis (Bogomolni and Spudich 1982). In 1985, a second photosensory rhodopsin, named sensory rhodopsin II [SRII, also called phoborhodopsin (pR)], was identified in the same archaeon *H. salinarum* as a receptor only for negative phototaxis (Takahashi et al. 1985). These two sensory rhodopsins, *H. salinarum* SRI (HsSRI) and *H. salinarum* SRII (HsSRII), form tight signaling complexes with their cognate two-TM domain proteins, halobacterial transducer protein I (HtrI) and II (HtrII), respectively, in the cellular membrane with a 2:2 stoichiometry (Inoue et al. 2013b). In 2006, we succeeded in the conversion of HsBR into an SRII-like negative phototaxis sensor, where three amino acid residues of HsBR, namely Pro200, Val210 and Ala215, were replaced by the corresponding residues for SRII from the archaeon *Natronomonas pharaonis* (NpSRII), namely Thr, Tyr and Thr, respectively (Fig. 2d) (Sudo and Spudich 2006). Two of the substitutions of HsBR, P200T and V210Y, are essential for the interaction with HtrII through hydrogen bonds with Glu43, Ser62 and Thr74 of HtrII (Sudo et al. 2006). The other substitution, A215T, is a prerequisite for the steric hindrance in the early K-intermediate between the C_{14}–H group in the isomerized retinal chromophore and the introduced Thr residue (Sudo et al. 2005a, 2007). The stored energy due to the steric hindrance induces conformational changes in the M-intermediate, leading to the activation of HtrII (Klare et al. 2004; Moukhametzianov et al. 2006). The successful functional conversion provides critical information about the light–signal transduction mechanism in the SRII–HtrII complex and also implies a tight evolutionary relationship between an H^+ pumping rhodopsin and a photosensory rhodopsin, in spite of the amino acid sequence differences between HsBR and NpSRII (identity = 27%, similarity = 68%). In 2011, we characterized a novel rhodopsin named middle rhodopsin (MR) as an evolutionarily transitional form between HsBR and NpSRII (Fig. 1b) (Sudo et al. 2011a), in which a critical Thr residue (T204 in NpSRII) is conserved in MR, but two residues essential for the interaction with HtrII are not. Based on these results and those of other studies, we concluded that the insertion of the critical Thr residue occurred in an early step of the evolution from HsBR into NpSRII (Sudo et al. 2011a).

G-protein activator

Animal type-2 rhodopsins show no amino acid sequence homology with microbial type-1 rhodopsins, although both types of rhodopsins are commonly composed of seven TM domain helices and the chromophore retinal. In the dark, while microbial rhodopsins mainly have all-*trans* retinal as the chromophore, 11-*cis* retinal is contained in animal rhodopsins. Upon light absorption, excited animal rhodopsins are converted to metarhodopsin-II (Meta-II) through several photointermediates, including photorhodopsin, bathorhodopsin, lumirhodopsin and metarhodopsin-I (Shichida and Imai 1998). The structural rearrangement of the cytoplasmic halves of TM helices 5 and 6 occurs on Meta-II; for activation, the exposed residues on the helices and loops interact with a type of heterotrimeric G-protein, transducin (G_t) (Ye et al. 2010; Choe et al. 2011), whereby the guanosine diphosphate–guanosine triphosphate (GDP–GTP) exchange reaction is induced (Shichida and Imai 1998; Ernst et al. 2014). A similar structural change of TM helices 5 and 6, referred to as the "helix opening," is also observed for microbial type-1 rhodopsins such as HsBR and NpSRII (Subramaniam et al. 1993; Oka et al. 2000; Wegener et al. 2001; Shibata et al. 2010). However, little or no G-protein activation is observed for microbial type-1 rhodopsins, suggesting the importance of the cytoplasmic loop for G-protein binding and/or GDP–GTP exchange reaction (Geiser et al. 2006; Nakatsuma et al. 2011; Sasaki et al. 2014). Animal type-2 rhodopsins are a member of the G-protein-coupled receptor (GPCR) family, in which differences in cytoplasmic loops are important to determine the selectivity for heterotrimeric G-protein activation (Yamashita et al. 2000). OptoXRs, the chimeric proteins of bovine rhodopsin (Rh) in which the cytoplasmic loops are replaced with those of the G_s-coupled hamster β_2-adrenergic receptor (β_2AR) and the G_q-coupled human α_{1a}-adrenergic receptor (α_{1a}AR), showed light-dependent activation of intracellular G_s and G_q, respectively (Airan et al. 2009). These OptoXRs are new types of optogenetic tools, and the reward-related behaviors of mice could be controlled by the optical activation of OptoXR when they were expressed in accumbens neurons (Airan et al. 2009). However, since the Schiff-base linkage of Meta-II thermally breaks during the decay process and the retinal is released from the protein moiety (opsin), multiple photoactivation of OptoXRs with repeated light illumination is considered to be difficult.

Geiser et al. reported that a chimeric HsBR, in which the third cytoplasmic loop was replaced with that of Rh, showed a light-dependent G_t activation (Geiser et al. 2006). Since HsBR shows a photocyclic reaction upon light illumination, this chimeric HsBR enables the multiple photo-activation of G_t without any bleaching of protein. However, the activation efficiency of the G_t of the chimera was very small (~ 37,000-fold lower than that of Rh) (Nakatsuma et al. 2011) and, therefore, it was difficult to apply it for optogenetics. On the basis of that background, we reported that NpSRII showed a G_t-activation function by replacing its third cytoplasmic loop with that of Rh (Nakatsuma et al. 2011), which had a similar efficiency to the HsBR/Rh chimera (30,000–14,000-th of Rh). In contrast, while a higher activation efficiency was achieved for the chimera between the eubacterial H^+ pump *Gloeobacter* rhodopsin (GR) and Rh (Fig. 2e) (Sasaki et al. 2014). The activation efficiency of the GR/Rh chimera was further enhanced by the

substitution of Glu132 with a glutamine residue (E132Q). E132Q is known to prolong the lifetime of the O-intermediate of GR (Miranda et al. 2009), and this was also shown for the GR/Rh + E132Q chimera by laser flash photolysis (Sasaki et al. 2014). In that study, we showed that there is a correlation between the G_t activation efficiencies and the lifetime of the O-intermediate for various types of chimeras, indicating the importance of the long-lived intermediate state for G-protein activation (Sasaki et al. 2014). Finally, we developed a double loop GR/Rh + E132Q chimera with the second and third cytoplasmic loops of Rh that showed the highest activation efficiency (3200-th of Rh and 64-th of G_o-coupled rhodopsin) (Fig. 2e) (Sasaki et al. 2014). Fourier transform infra-red (FTIR) spectroscopic analysis showed that the amide-I band of the G_t-activating chimera undergoes a larger change upon light activation than do the microbial rhodopsins without G_t activation ability (Sasaki et al. 2014). Since the outward movement of TM 6 in Meta-II of Rh is essential for G_t activation (Farrens et al. 1996; Choe et al. 2011), the larger change of amide-I for the GR/Rh chimera suggests that a similar conformational change of TM 6 occurs during its activation process. Thus, the successful functional conversion from microbial type-1 rhodopsins into the G-protein activator revealed the relationship between the two types of rhodopsins, in spite of their lack of amino acid sequence homology.

Conversion of other ion pumps

Archaeal proton and chloride pumps

The proton acceptor and donor in HsBR are Asp85 and Asp96, respectively, and they play a critical role in the H^+ transport with Thr89. These three residues are called the "DTD-motif" (Béjà and Lanyi 2014; Inoue et al. 2014a), and in HsHR this motif is replaced by the "TSA-motif." As described above, when Asp85 (the first D of the DTD-motif) of HsBR is mutated to Thr, the D85T mutant is able to pump Cl^- inwardly, as does HsHR (Figs. 2a, 3a) (Sasaki et al. 1995; Tittor et al. 1997). This observation implies that HsBR and HsHR share a common transport mechanism and that their ion selectivity is determined at the position of the primary proton acceptor (Asp85 in HsBR). While this was a clear-cut result, the reverse substitution (i.e. Thr → Asp) did not convert HsHR into an H^+ pump (Havelka et al. 1995; Váró et al. 1996). Nine additional substitutions of a homologous protein of HsHR, *Natronomonas pharaonis* HR (NpHR), also did not convert it to a H^+ pump, indicating that the direction of functional conversion between H^+ and Cl^- pumps is asymmetric (Fig. 3a) (Muroda et al. 2012). FTIR spectroscopic analysis suggested that protein-bound water molecules may be related to the asymmetric functional conversion (Muroda et al. 2012).

Eubacterial proton, sodium and chloride pumps

In 2000, a new class of outward H^+ pump was found in an uncultured marine bacterium and was named proteorhodopsin (PR) (Fig. 1b) (Béjà et al. 2000). In this new outward H^+ pump the proton donor of HsBR (Asp96) is replaced with a Glu residue. Thus, PR has a DTE-motif instead of the DTD-motif of HsBR in helix C. Many homologous DTE-type H^+ pumping microbial rhodopsins have since been found in various eubacterial species, including xanthorhodopsin (XR), which binds an antennae carotenoid (salinixanthin) on the outer side of the TM region of helices E, F and G (Balashov and Lanyi 2007), *Gloeobacter* rhodopsin (GR) (Miranda et al. 2009) and thermophilic rhodopsin (TR) from the extreme thermophile *Thermus thermophilus* (Fig. 1b) (Tsukamoto et al. 2013). In addition, the eubacterial light-driven Na^+ and Cl^- pumps *Krokinobacter eikastus* rhodopsin 2 (KR2) and *Fulvimarina* rhodopsin (FR), respectively, were discovered in 2013 and 2014, respectively (Inoue et al. 2013a, 2014b; Yoshizawa et al. 2014), and they form new phylogenetic clades (Fig. 1b). KR2 and FR have an NDQ-motif (Asn, Asp and Gln) and an NTQ-motif (Asn, Thr and Gln) at positions homologous to the DTD-motif and the DTE-motif of HsBR and PR, respectively (Inoue et al. 2014a). These three types of eubacterial ion pumping rhodopsins (H^+, Na^+ and Cl^-) provided the possibility of six functional conversions among them (i.e. $H^+ \Leftrightarrow Cl^-$, $H^+ \Leftrightarrow Na^+$, $Na^+ \Leftrightarrow Cl^-$) (Fig. 3b). As the motifs of eubacterial rhodopsins are likely to determine their functions, we examined these functional conversions by altering them for GR (H^+ pump), KR2 (Na^+ pump) and FR (Cl^- pump). Among those six potential functional conversions, only one conversion was actually functional, from a Na^+ to a H^+ pump (Inoue et al. 2016b). This may be consistent with the fact that KR2 transports H^+ in the absence of Na^+ (Inoue et al. 2013a), which suggests that KR2 retains the molecular machinery of a H^+ pump in its structure. However, the H^+ transport efficiency of the DTE mutant of KR2 (N112D/D116T/Q123E) was less than the efficiency of the natural H^+ pumping rhodopsins, especially in solutions containing NaCl, but it was enhanced in solutions containing CsCl, which implies that Na^+ inhibits H^+ transport in the DTE mutant of KR2. As the Asp102 of KR2, which is characteristic of Na^+ pumps, constitutes the Na^+ binding site in the crystal structure (Gushchin et al. 2015; Kato et al. 2015a), we replaced that residue with the neutral residue Asn. The DTE/D102N mutant of KR2 exhibited high H^+ pumping activities even in solutions containing NaCl. Thus, the functional conversion of the $Na^+ \rightarrow H^+$ pump was achieved by four mutations (top panel in Fig. 3b). In contrast, the reverse motif mutation in GR from DTE to NDQ was not enough to produce a Na^+ pumping rhodopsin even if all six mutations were introduced (top panel in Fig. 3b), implying that additional substitutions are required to make this functional conversion successful.

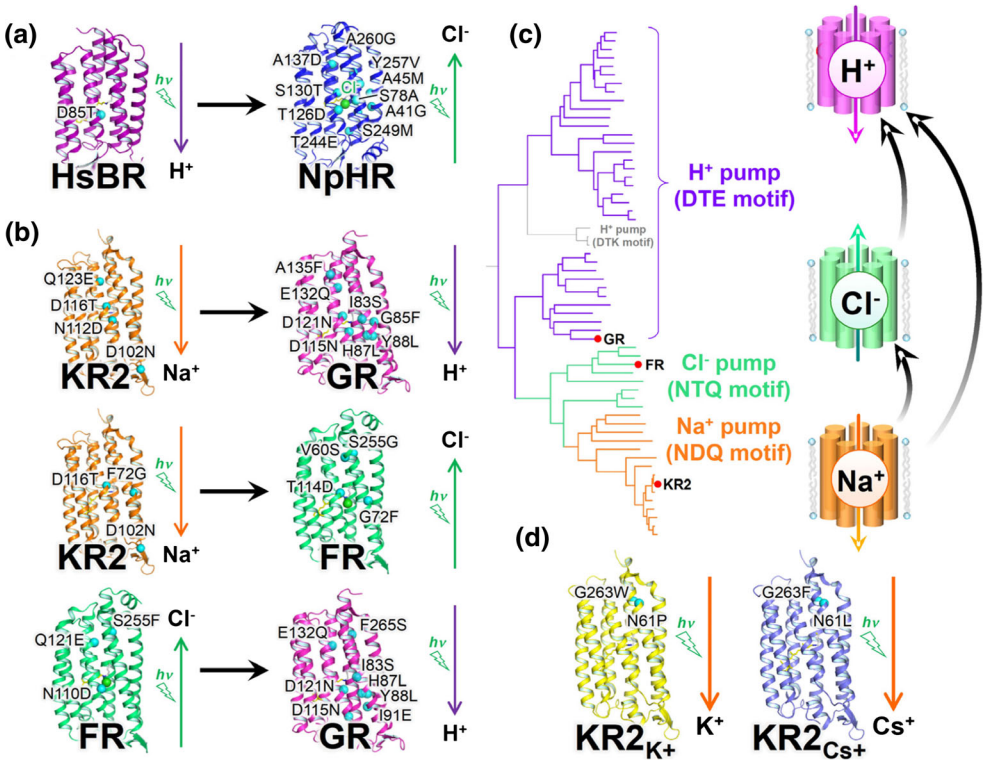

Fig. 3 Schematics of conversion among ion pumps. **a** Asymmetric functional conversion of the archaeal light-driven ion pumps HsBR (H^+ pump) and *Natronomonas pharaonis* halorhodopsin (NpHR; PDB ID 347K; Cl^- pump) (Kouyama et al. 2010). **b** Asymmetric functional conversion of eubacterial light-driven ion pumps GR (H^+ pump), *Krokinobacter eikastus* rhodopsin 2 (KR2; Na^+ pump) and *Fulvimarina* rhodopsin (FR; Cl^- pump). The structures of GR, KR2 and FR are illustrated by reference to the crystal structures of XR (PDB ID 3DDL, a homologous protein of GR), KR2 (PDB ID 3X3C) and NmClR (PDB ID 5B2N, a homologous protein of FR) (Hosaka et al. 2016), respectively. **c** Phylogenetic tree of eubacterial light-driven ion pumps and the asymmetric results of functional conversions among them. **d** Creations of new classes of light-driven ion pumps through the modification of the residues of eubacterial light-driven Na^+ pump KR2. The structure of KR2 is illustrated by reference to its crystal structure (PDB ID 3X3B). For all panels, the membrane is roughly in the vertical plane of these images, and the top and bottom regions correspond to the cytoplasmic and extracellular sides, respectively

Next, we examined the functional conversion between Na^+ and Cl^- pumps using KR2 and FR. As the simple motif replacement for the Na^+ pump KR2 (NDQ → NTQ, i.e. D116T) resulted in an unsuccessful $Na^+ \rightarrow Cl^-$ pump conversion, we suspected that the negatively charged Na^+ binding site in KR2 (Inoue et al. 2013a; Gushchin et al. 2015; Kato et al. 2015a) prevents inward Cl^- pumping. That is indeed the case, as the D116T(NTQ)/D102N mutant of KR2 exhibited a robust light-induced Cl^- transport activity (middle panel in Fig. 3b). Furthermore, we focused on Phe72 in helix B of KR2 because that residue is located near the Schiff base region and is highly conserved among the Cl^- pumps. The D116T(NTQ)/F72G/D102N mutant of KR2 showed a larger light-induced Cl^- pumping activity than did the D116T(NTQ)/D102N mutant (Inoue et al. 2016b). We then examined a reverse $Cl^- \rightarrow Na^+$ pump conversion, but the simple motif replacement for the Cl^- pump FR (NTQ → NDQ, i.e. T114D) resulted in an unsuccessful conversion. To make that conversion possible, we constructed a variety of additional mutants, including V60S and S225G (middle panel of Fig. 3b), but none of these mutants showed any ion transport activity. Thus, while the $Na^+ \rightarrow Cl^-$ pump conversion was successful, the reverse $Cl^- \rightarrow Na^+$ pump conversion can not yet be achieved, showing an asymmetric interconversion (middle panel in Fig. 3b).

For the $H^+ \Leftrightarrow Cl^-$ interconversion between GR and FR, the motif replacement mutations (DTE ⇔ NTQ) were not sufficient for functional conversions. Therefore, we introduced an additional four mutations to the GR NTQ mutant (GR NTQ/I83S/H87S/D115N/F265S) to make a Cl^- pump (Fig. 3b). However, that mutant did not show any Cl^- pumping function. The Cl^- ion commonly binds near the Schiff base nitrogen as a counterion of Cl^- pumps, such as HsHR, NpHR, FR and a Cl^- pumping KR2 mutant (KR2 NTQ/F72G/D102N), but the GR mutant does not bind Cl^-. Therefore, we consider that a proper structure required for Cl^- binding site is not achieved by these mutations and that this is the main reason why we observed no Cl^- transport activity for the GR mutant. We then tried to optimize the functional conversion from Cl^- to H^+ pumps. Gly263 of Na^+ pump KR2 is a key residue for Na^+ uptake (Gushchin et al. 2015; Kato et al. 2015a). The corresponding amino acids are Ser and Phe for FR and GR, respectively, which may be important for the ion specificity of each pump.

Indeed, the results showed that the FR DTE/S255F mutant functions as an outward H^+ pump. We thus conclude that the functional interconversion for the $H^+ \Leftrightarrow Cl^-$ pair is asymmetric as well (bottom panel in Fig. 3b).

Figure 3c shows a phylogenetic tree of eubacterial ion pumping rhodopsins and the asymmetric results of functional conversions. Of note, only one functional conversion in each pair of proteins was possible, whereas the reverse conversions did not work. Here we discuss the asymmetric interconversions from the evolutionary viewpoint. Based on the conserved helix C motif, eubacterial rhodopsins can be classified into DTX (H^+ pumps; X is mostly E), NTQ (Cl^- pumps) and NDQ (Na^+ pumps) rhodopsins, which are distinct from haloarchaeal DTD (H^+ pumps) and TSA (Cl^- pumps) rhodopsins. This phylogenetic relationship strongly suggests that the ancestor of eubacterial ion pump rhodopsins is an H^+ pump, from which Cl^- pumps emerged, followed by the appearance of Na^+ pumps (Fig. 3C). Successful functional conversions are attained exclusively when the mutagenesis attempts to reverse the course of evolution, but not when it follows the evolutionary direction (Inoue et al. 2016b). Dependence of the observed functional conversions on the direction of evolution strongly suggests that the essential elements of an ancestral function are retained even after the gain of a new function, while the gain of a new function needs the accumulation of multiple mutations, which may not be easily reproduced by limited mutagenesis in vitro.

It should be noted that the asymmetric functional interconversion between eubacterial H^+ and Cl^- pumps (GR and FR) is opposite that between archaeal H^+ and Cl^- pumps, where the $H^+ \rightarrow Cl^-$ pump conversion was achieved by a single amino acid substitution (Sasaki et al. 1995; Tittor et al. 1997), but the reverse conversion was unsuccessful (Havelka et al. 1995; Váró et al. 1996; Muroda et al. 2012). If the success of functional conversion of ion-pumping rhodopsins depends on the direction of evolution, how can the results of the archaeal H^+ and Cl^- pumps be explained? The phylogenetical analysis of archaeal ion pumps is less hierarchical than that for eubacterial pumps, with much older branching. Thus, a different molecular mechanism, such as the hydrogen-bonding strength of protein-bound water molecules (Muroda et al. 2012) underlies the asymmetric functional conversion in archaeal H^+ and Cl^- pumps. Recently, a new class of Cl^- pump, which has a TSD-motif, was reported from cyanobacterium *Mastigocladopsis repens* (MrHR) (Hasemi et al. 2016) and *Synechocystis* sp. PCC 7509 (SyHR) (Niho et al. 2017). This pump retains the aspartic acid homologous to the H^+ donor of archeal H^+ pumps (Asp96 in HsBR). The mutation of Thr74 to Asp in MrHR (i.e. changing the motif from TSD to DTD) converted the function to a H^+ pump (Hasemi et al. 2016). Although the phylogenetical distance between MrHR and HsBR is similar to that between HRs (HsHR and NpHR) and HsBR (Fig. 1b), for which the conversion of a Cl^- pump to a H^+ pump was impossible (Muroda et al. 2012), the functional conversion by a single amino acid substitution suggests that structural and functional elements required for the H^+ pump are conserved in MrHR, but not in archeal HRs.

Non-natural ion pump

In addition to the functional conversion between ion pumps existing in nature, new classes of ion pumps have been created by modifying the residues of the Na^+ pump KR2. The crystal structure of KR2 has an intramolecular hydrophilic cavity ("intracellular vestibule" or "ion uptake cavity") on the cytoplasmic side (Gushchin et al. 2015; Kato et al. 2015a). This cavity has a bottle-neck-like structure in the middle part of the TM region and is composed of several amino acid residues, including Asn61 and Gly263. We have shown that the mutant of KR2 for these residues (N61P/G263W named "$KR2_{K+}$") shows K^+ transport activity (Fig. 3d) (Kato et al. 2015a). Furthermore, by screening the 12 types of mutations, we obtained a Cs^+-transporting KR2 (N61L/G263F named "$KR2_{Cs+}$") (Fig. 3d) (Konno et al. 2016). Thus, it is now possible to produce artificial ion pumps by atomistic design of the mutation.

Conversion of cation channels

In native cells, ChRs work as sensors for phototaxis behavior via changes in motility mediated through their light-gated cation channeling function (Sineshchekov et al. 2002). These ChRs not only have biological significance, but when they are heterologously expressed in animal neurons they evoke an action potential upon light illumination. This property enables the temporally and spatially precise control of neural activation to be used as a genetically encoded tool for optogenetics (Boyden et al. 2005; Deisseroth 2015), with CrChR2 being one of the most widely used optogenetic tools. Thus, from the biological and technological points of view, the ion-transporting mechanisms of ChRs have been extensively studied by various biophysical methods (Ritter et al. 2008; Radu et al. 2009; Eisenhauer et al. 2012; Lórenz-Fonfría et al. 2013; Ito et al. 2014; Lórenz-Fonfría et al. 2014; Muders et al. 2014). For most ChRs, a glutamic acid at the homologous position of Asp85 of HsBR is conserved as the counterion, whereas an acidic residue at the position of Asp96 of HsBR, a proton donor of the deprotonated Schiff base for proton pumps, is not conserved. On the basis of that background and the crystallographic structure of C1C2, two research groups successfully produced anion-conducting rhodopsins by mutating several residues of ChRs (Fig. 4) (Berndt et al. 2014; Wietek et al. 2014). Based on theoretical studies one group predicted that the replacement of Glu90 in

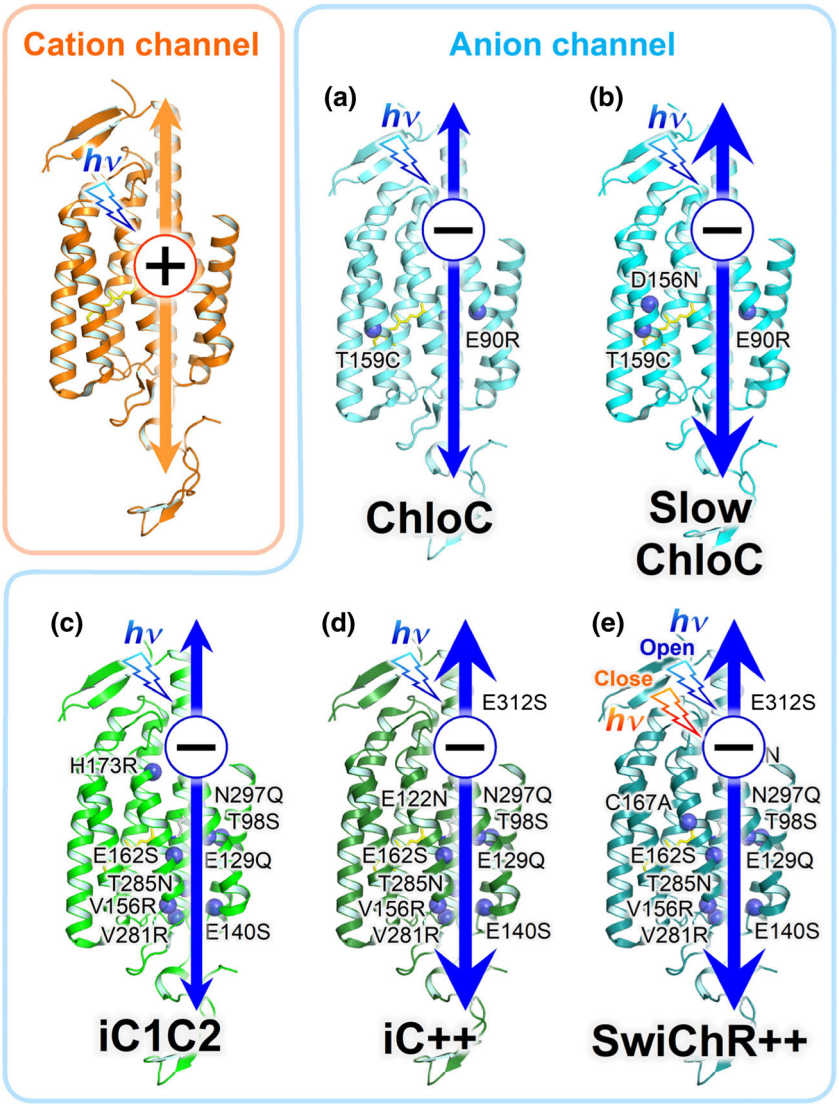

Fig. 4 Conversion of the channelrhodopsin (ChR) light-gated cation channels. **a**, **b** Conversion of a light-gated cation channel (CrChR2) into light-gated anion channels (ChloC and slowChlo) by two and three amino acid substitutions, respectively. **c**, **d** Conversion of a light-gated cation channel (C1C2) into light-gated anion channels (iC1C2 and iC++) by nine and ten amino acid substitutions and replacing the C-terminus with that of CrChR2, respectively. **e** Conversion of a light-gated cation channel (C1C2) into a bistable light-gated anion channel (SwiChR++) that can open and close the ion transport pathway when exposed to blue and red light pulses, respectively. The structures for all panels are constructed on the basis of the crystal structure of C1C2 (PDB ID 3UG9). The membrane normally is roughly in the vertical plane of these images, and the top and bottom regions correspond to the cytoplasmic and extracellular sides, respectively

CrChR2 (corresponding to Ala53 in HsBR) by lysine or arginine would show permeation of Cl^- ions inside the protein (Wietek et al. 2014). Actually, the E90R mutant of CrChR2 in combination with T159C (named ChloC) showed a significant Cl^--channeling function (Fig. 4a) (Wietek et al. 2014). Furthermore, by mutating Asp156 of the mutant (ChloC) to an asparagine (ChR2 E90R/D156N/T159C, slowChloC), the lifetime of the channel opening was strongly enhanced and a large photocurrent even with a shorter light pulse was obtained (Fig. 4b). The other research group designed another type of anion-conducting ChR by site-directed mutations of C1C2. A multiple mutant of C1C2 (named iC1C2, Fig. 4c) was shown to have a sufficiently large photocurrent, representing anion conductance (Berndt et al. 2016). The conductance (photocurrent) of iC1C2 was increased by optimizing the mutation sites and replacing the C-terminus with that of CrChR2 (iC++; Fig. 4d) (Berndt et al. 2016). The time of channel closing in the mutant (iC++) was decelerated by 9500-fold by mutating Cys128 to an alanine. This mutant (named SwiChR++) showed a step-function type photocurrent, where it is opened by a blue light pulse and is immediately closed by a red light pulse (Fig. 4e) (Berndt et al. 2016). These artificial anion channels are expected to be useful in optogenetics as a neural silencer. Thus, the successful functional conversion by substitutions of multiple amino acids revealed that the essential differences between cation and anion channels are far less than previously imagined. Recently, the Spudich group reported a new class of natural anion-conducting ChRs (ACRs) from the eukaryotic alga *Guillardia theta* (Govorunova et al. 2015). Among the three ACR genes existing in the genome of *G. theta* (GtACR1, 2 and 3), two (GtACR1 and GtACR2) showed anion transport activity in transfected human embryonic kidney (HEK293) cells (Govorunova et al. 2015) (Fig. 1b). While the maximum wavelength of the action spectrum of GtACR1 is located around 515 nm (green absorbing), GtACR2 showed a blue-shifted maximum at 470 nm (blue

absorbing). Natural ACRs showed a larger (several nA) photocurrent and a stronger inhibition of the generation of action potential by light than those of ChR-based anion channels (Govorunova et al. 2015). We recently demonstrated that the ion transport activity of GtACR2 is strongly (10-fold) enhanced by a mutation of the conserved Arg residue (R84E) located on a loop (the B-C loop) between TM helix 2 and TM helix 3, when it is expressed in *Escherichia coli* cells as a recombinant protein (Doi et al. 2017). In the future, further modification(s) will be applied to natural ACRs to obtain efficient neural silencers.

Conversion of photosensors

Proton pump

Microbial phototaxis receptors, such as HsSRI and HsSRII, form complexes with cognate transducer proteins HtrI and HtrII on cellular membranes (Inoue et al. 2013b). HsSRI and HsSRII induce conformational changes upon illumination, and they transmit signals to HtrI and HtrII, respectively. HtrI and HtrII then relay the signals to downstream molecules such as CheA and CheY (Hoff et al. 1997). Eventually, the phosphorylated CheY binds to the flagellar motor and changes its rotation pattern, resulting in phototaxis responses (Fig. 5) (Hoff et al. 1997). HsSRI has an absorption maximum at 587 nm, and it therefore absorbs orange light. Light illumination of HsSRI triggers *trans–cis* isomerization of the retinal chromophore, leading to the sequential appearance of several intermediates during the photocycle, such as K-, L- and M-intermediates, where the M-intermediate is an active form for the positive phototaxis responses (Swartz et al. 2000). The M-intermediate shows an absorption maximum at 373 nm and absorbs blue light. When the M-intermediate receives blue light, it is converted into P_{520}, an active form for negative phototaxis responses (Spudich and Bogomolni 1984). Thus, HsSRI is responsible for both negative and positive phototaxis in collaboration with HtrI. On the other hand, HsSRII and its homologous protein from the archaeon *N. pharaonis* (NpSRII) have absorption maxima at 487 and 498 nm, respectively, and they work as negative phototaxis sensors for blue light (Takahashi et al. 1990; Imamoto et al. 1992). Illumination of HsSRII and NpSRII with blue light leads to the appearance of several intermediates (K-, L-, M- and O-intermediates) during the photocycle (Imamoto et al. 1992), where the long-lived M- and O-intermediates are considered to be active forms for negative phototaxis (Yan et al. 1991). Those signals are relayed to HtrII through both the membrane-spanning and the cytoplasmic domains of SRII (Sudo et al. 2005b; Moukhametzianov et al. 2006).

Although the identities of amino acid residues between SRs and HsBR are low (HsBR–HsSRI: 26%, HsBR–HsSRII: 30%, HsBR–NpSRII: 27%), the blue-shifted M-intermediate is commonly formed during the photocycle of HsSRI, HsSRII and NpSRII. In the case of HsBR, a proton of the protonated Schiff base is transferred to its counterion Asp85 upon formation of the M-intermediate, and the proton transfer reaction is crucial for the H^+ pump function of HsBR (Mogi et al. 1988). By analogy, it is expected that SRs have a potential to show proton pumping activity. However, when HsSRI, HsSRII and NpSRII are functionally co-expressed with their cognate transducer proteins, they form tight complexes in the membrane, and no net proton transport pumping activity is observed (Bogomolni et al. 1994; Sasaki and Spudich 1999; Sudo et al. 2001a). In contrast, HtrI-free HsSRI and HtrII-free NpSRII have robust proton pumping activities (Fig. 5a) (Bogomolni et al. 1994; Sudo et al. 2001b), implying that the proton pumping mechanism of HsBR is conserved in sensory rhodopsins, HsSRI and NpSRII. Thus, these results reveal an evolutionary relationship between ion pumping rhodopsins

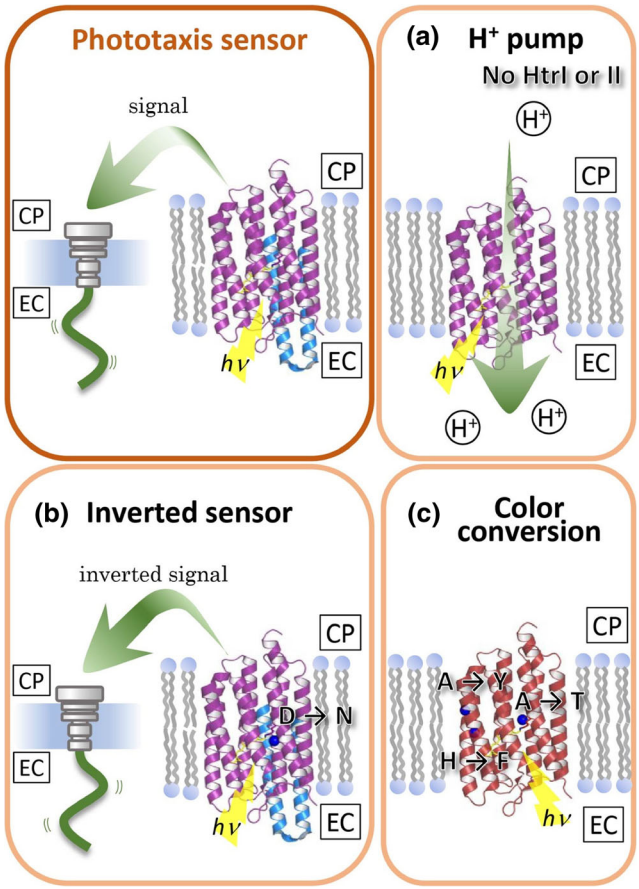

Fig. 5 Conversion of photosensory rhodopsins. **a** Conversion of the phototaxis sensory rhodopsins (SR) HsSRI and NpSRII into light-driven outward proton pumps by the removal of cognate transducer proteins, HtrI and HtrII. **b** Conversion of the phototaxis sensory rhodopsin HsSRI into an inverted phototaxis sensor by a single amino acid substitution (D201N). **c** Conversion of the phototaxis sensory rhodopsin SrSRI into a blue-shifted one by three amino acid substitutions (H131F/A136Y/A200T). The structures for all panels are from the complex of NpSRII (purple) and HtrII (blue) (PDB ID 1H2S)

and photosensory rhodopsins, in spite of their amino acid sequence differences.

Functional inversion

The active center of the proton pump HsBR is composed of deprotonated Asp85, deprotonated Asp212, protonated Arg82 and water molecules and their hydrogen bonds (Lanyi 2004). Asp212 is called the secondary counterion and stabilizes the protonated Schiff base with the primary counterion Asp85. As well as Asp85, Asp212 is essential for the H^+ pumping function of HsBR (Mogi et al. 1988). In 1995, it was reported that the substitution of Asp201 of HsSRI (Asp212 of HsBR) with the neutral residue Asn (D201N) converted the attractant signaling function to a repellent signaling one (Fig. 5b) (Olson et al. 1995). D201N exhibited a greatly altered photocycle in which Schiff base deprotonation (i.e. M-intermediate formation) is greatly reduced, indicating the importance of Asp201 not only for proton pumping, but also for the photosensing. Because the M-intermediate of HsSRI produces the P_{520} intermediate necessary for negative phototaxis upon UV-light illumination (Spudich and Bogomolni 1984), it is likely that the structure of the unphotolyzed state of the D201N mutant is similar to that of the M-intermediate of HsSRI. On the basis of these results and other findings, Spudich et al. proposed an opposite conformational two-state model for the attractant and repellent signaling behavior of the SR–Htr complexes, in which the Schiff base connectivity is switched from/to inward/outward to from outward/inward (Sineshchekov et al. 2008). Thus, the successful functional conversion of HsSRI by a single amino acid substitution revealed that essential differences between positive and negative phototaxis sensors are far less than imagined.

Color variant

Although both SRI and SRII work as phototaxis receptors, their respective absorption maxima differ considerably. For example, the absorption maxima of HsSRI and NpSRII are located at 587 and 498 nm, respectively. To analyze the color tuning mechanisms in SRs, we attempted to produce a blue-shifted SRI (Sudo et al. 2011b). Because HsSRI is unstable, especially in the detergent-solubilized state without NaCl, we employed a homologous protein from the eubacterium *Salinibacter ruber* (SrSRI) (Fig. 1b), which is much more stable and could be expressed as a recombinant protein in *Escherichia coli* cells (Kitajima-Ihara et al. 2008). By comparing amino acid sequences of SRs, we found several candidate residues for color tuning, and they are mutated in SrSRI. Finally, the triple mutant of SrSRI (H131F/A136Y/A200T) exhibited a large spectral blue-shift from 557 to 525 nm (Fig. 5c) (Sudo et al. 2011b). We also confirmed that the inverse mutant of NpSRII shows a large spectral red-shift in contrast to SrSRI (Sudo et al. 2011b). One of the substitutions of SrSRI, H131F, is related to the Cl^- binding near the β-ionone ring of the retinal chromophore. We previously reported that Cl^- binding is widely conserved among the SRI protein family (Suzuki et al. 2009; Yagasaki et al. 2010). In the electronic ground state of rhodopsins, a positive charge of the retinal chromophore is localized mainly on the Schiff base nitrogen, and it shifts toward the β-ionone ring upon excitation (Katayama et al. 2015). Similarly, a positive charge located on the Schiff base nitrogen is likely to move to the β-ionone ring by Cl^- binding to His131 of SrSRI by electrical interaction, leading to the spectral blue-shift. One of the mutated residues of SrSRI, Ala136, is also located near the retinal β-ionone ring, while another of them, Ala200, is located near the Schiff base region. The changes in charge distribution of the retinal chromophore and/or steric hindrance by these mutations would cause changes in factors (1), (2) and/or (3) discussed in subsection Color variant of section Conversion of the outward proton pump section.

Future directions

Microbial rhodopsins have been extensively studied from 1971 to the present, and the basic knowledge obtained has allowed researchers to convert the biological functions of various microbial rhodopsins. Successful functional conversion provides information on functionally essential elements that has difficult to obtain using only individual rhodopsin molecules (Fig. 6a). Such information has resulted in microbial rhodopsins becoming one of the frontrunners of research on both photoactive proteins and membrane-embedded proteins. Some of the mutated residues for the functional conversion of microbial rhodopsins are located around the retinal chromophore (< 5 Å), indicating that the active center is composed of the retinal chromophore and nearby amino acid residues, water molecules and ions (Fig. 6a). The retinal-binding cavity in microbial rhodopsins is regarded as a substrate-binding cavity in other receptor proteins and, therefore, functional conversion is a useful strategy to gain an understanding of the active center of biological molecules. Noteworthy, some of the residues necessary for the functional conversion of microbial rhodopsins are located at a region far from the retinal chromophore (> 5 Å) (Fig. 6a). For ion transporters, including some of the microbial rhodopsins, the alternating access model is thought to be a fundamental mechanism (Slotboom 2014; Drew and Boudker 2016). In this model, protein structures are altered from the inward or outward facing states to the outward or inward facing states upon stimulation with changes in the affinity of the cognate ions. Therefore, mutated residues far from the retinal chromophore are thought to be composed of the ion transport pathway (Figs. 3b, d, 4). For sensors, however, interaction sites for the cognate transducer

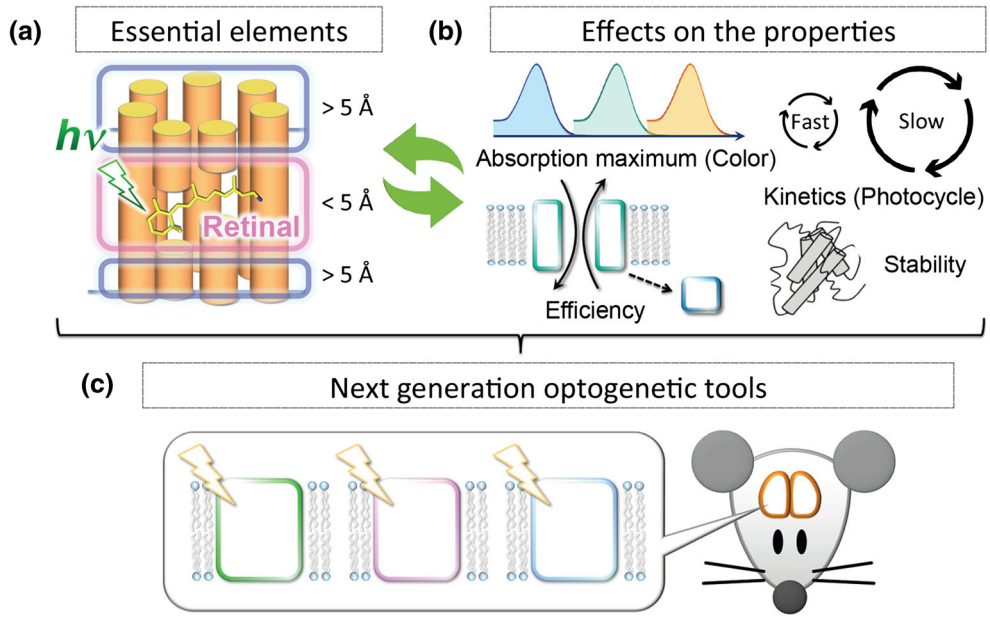

Fig. 6 Future directions of microbial rhodopsin research. **a** Conversion among microbial rhodopsins provides critical information about functionally essential elements located near the retinal chromophore (< 5 Å) and far from the retinal chromophore (> 5 Å). **b** Functional conversion also affects other molecular properties, such as color, efficiency, kinetics and stability, which will be further investigated in the future to make rationally designed molecules. **c** Knowledge obtained from **a** and **b** will allow the development of novel optogenetic tools

proteins, such as Htrs and G-proteins, are located on the protein surface and are essential for signal transduction (Fig. 2d, e). Therefore it is reasonable to conclude that the mutated residues are far from the retinal chromophore, which is located at the middle of the TM helices. Thus, in addition to the active center, functional conversion also identifies regions involved in the biological functions on the protein surface (Fig. 6a). This conclusion can also be extrapolated not only to other photoactive proteins and membrane-embedded proteins, but also to many other biological molecules.

Of note, in addition to changes in biological activities (i.e. ion transport and signal transduction), functionally converted mutant proteins also had changes induced in their molecular properties, such as absorption maximum, efficiency, kinetics and stability (Fig. 6b). The native rhodopsins have been optimized by nature for a long time. Therefore, in addition to the functionally essential region, modifications to other regions to maintain and/or alter such molecular properties have occurred during the evolutionary process. Actually, there is a wide variety of amino acid sequences among microbial rhodopsins (identity: 11 ~ 48%, similarity: 43 ~ 76%). Thus, the functionally converted mutant proteins should be further modified to fully understand the biological functions of microbial rhodopsins (Fig. 6b). For these modifications, research on rhodopsins showing a variety of such properties (absorption maxima, efficiency, kinetics and stability) would be useful. As a representative example, we recently identified a few rhodopsins with extremely high thermal stability (Tsukamoto et al. 2013; Honda et al. 2017; Kanehara et al. 2017) and solved one of their crystal structures (Tsukamoto et al. 2016). Combining experimental results with molecular simulations, some regions responsible for the high stability were estimated, and we are planning to insert that region into thermally unstable rhodopsins, such as HsSRI, to make them more stable. We expect that the stabilization mechanism of microbial rhodopsins can be applied to other membrane-embedded proteins, such as G-protein-coupled receptors, which are often unstable, especially in the detergent-solubilized state. Thus, microbial rhodopsins should be further investigated in detail not only to understand their molecular properties but also to utilize them as models for both photoactive proteins and membrane-embedded proteins.

In addition to the biological aspect of microbial rhodopsins, these molecules have received increased attention as a tool for optogenetics (Fig. 6c). Indeed, cation ChRs, such as CrChR2, and anion ChRs, such as GtACR1, are widely utilized as light-dependent neural activators and silencers, respectively, even in living animals (Boyden et al. 2005; Govorunova et al. 2015). As described above, on the basis of knowledge of the color tuning mechanism, we successfully produced blue-shifted color variants of rhodopsins without any loss of biological activity (Sudo et al. 2013; Kato et al. 2015b). Similarly, producing rationally designed rhodopsins with changes in absorption maximum, high efficiency, fast kinetics and high stability would also be useful for optogenetics. As an example, some research groups have attempted to make a red-shifted color variant, although the ion transport activity was not sufficient (Prigge et al. 2012; Lin et al. 2013). Both CrChR2 and GtACR1 absorb blue light (Nagel et al. 2003; Govorunova et al. 2015), which shows less tissue permeability due to the scattering and absorption of some molecules. Therefore, the optical fiber has to be inserted deeply in the brain. If a rhodopsin shows an absorption maximum above 800 nm, it would be possible to regulate rhodopsin function by light without insertion of the optical fiber (Fig. 6c). To this end, in addition to combinations of mutations, other strategies, such

as replacement of the retinal chromophore and addition of a secondary chromophore to use a two-photon process, would be useful.

In conclusion, the functional conversion of microbial rhodopsins provides a suitable approach not only for basic research but also for the development of next generation optogenetic tools.

Acknowledgements Our original publications were supported by a Grant-in-Aid from the Japanese Ministry of Education, Science, Technology, Sports and Cultures (KAKENHI) to KI, HK and YS. This work was also supported by JST-CREST and AMED to YS. We thank "DASS Manuscript" (http://www.dass-ms.com/home.html) for the English language review.

Compliance with ethical standards

Conflict of interest Akimasa Kaneko declares that he has no conflict of interest. Keiichi Inoue declares that he has no conflict of interest. Keiichi Kojima declares that he has no conflict of interest. Hideki Kandori declares that he has no conflict of interest. Yuki Sudo declares that he has no conflict of interest.

Ethical approval This article does not contain any studies with human participants or animals performed by any of the authors.

References

Airan RD, Thompson KR, Fenno LE, Bernstein H, Deisseroth K (2009) Temporally precise in vivo control of intracellular signalling. Nature 458:1025–1029

Avelar GM, Schumacher RI, Zaini PA, Leonard G, Richards TA, Gomes SL (2014) A rhodopsin-guanylyl cyclase gene fusion functions in visual perception in a fungus. Curr Biol 24:1234–1240

Béjà O, Aravind L, Koonin EV, Suzuki MT, Hadd A, Nguyen LP, Jovanovich SB, Gates CM, Feldman RA, Spudich JL, Spudich EN, DeLong EF (2000) Bacterial rhodopsin: evidence for a new type of phototrophy in the sea. Science 289:1902–1906

Béjà O, Lanyi JK (2014) Nature's toolkit for microbial rhodopsin ion pumps. Proc Natl Acad Sci USA 111:6538–6539

Balashov SP, Lanyi JK (2007) Xanthorhodopsin: proton pump with a carotenoid antenna. Cell Mol Life Sci 64:2323–2328

Berndt A, Lee SY, Ramakrishnan C, Deisseroth K (2014) Structure-guided transformation of channelrhodopsin into a light-activated chloride channel. Science 344:420–424

Berndt A, Lee SY, Wietek J, Ramakrishnan C, Steinberg EE, Rashid AJ, Kim H, Park S, Santoro A, Frankland PW, Iyer SM, Pak S, Ahrlund-Richter S, Delp SL, Malenka RC, Josselyn SA, Carlen M, Hegemann P, Deisseroth K (2016) Structural foundations of optogenetics: determinants of channelrhodopsin ion selectivity. Proc Natl Acad Sci USA 113:822–829

Bogomolni RA, Spudich JL (1982) Identification of a third rhodopsin-like pigment in phototactic *Halobacterium halobium*. Proc Natl Acad Sci USA 79:6250–6254

Bogomolni RA, Stoeckenius W, Szundi I, Perozo E, Olson KD, Spudich JL (1994) Removal of transducer HtrI allows electrogenic proton translocation by sensory rhodopsin I. Proc Natl Acad Sci USA 91: 10188–10192

Boyden ES, Zhang F, Bamberg E, Nagel G, Deisseroth K (2005) Millisecond-timescale, genetically targeted optical control of neural activity. Nat Neurosci 8:1263–1268

Braiman MS, Mogi T, Marti T, Stern LJ, Khorana HG, Rothschild KJ (1988) Vibrational spectroscopy of bacteriorhodopsin mutants: light-driven proton transport involves protonation changes of aspartic acid residues 85, 96, and 212. Biochemistry 27:8516–8520

Brown LS, Ernst OP (2017) Recent advances in biophysical studies of rhodopsins—oligomerization, folding, and structure. Biochim Biophys Acta 1865:1512–1521

Choe HW, Kim YJ, Park JH, Morizumi T, Pai EF, Krauss N, Hofmann KP, Scheerer P, Ernst OP (2011) Crystal structure of metarhodopsin II. Nature 471:651–655

Deisseroth K (2015) Optogenetics: 10 years of microbial opsins in neuroscience. Nat Neurosci 18:1213–1225

Doi S, Tsukamoto T, Yoshizawa S, Sudo Y (2017) An inhibitory role of Arg-84 in anion channelrhodopsin-2 expressed in *Escherichia coli*. Sci Rep 7:41879

Drew D, Boudker O (2016) Shared molecular mechanisms of membrane transporters. Annu Rev Biochem 85:543–572

Eisenhauer K, Kuhne J, Ritter E, Berndt A, Wolf S, Freier E, Bartl F, Hegemann P, Gerwert K (2012) In channelrhodopsin-2 Glu-90 is crucial for ion selectivity and is deprotonated during the photocycle. J Biol Chem 287:6904–6911

Ernst OP, Sanchez Murcia PA, Daldrop P, Tsunoda SP, Kateriya S, Hegemann P (2008) Photoactivation of channelrhodopsin. J Biol Chem 283:1637–1643

Ernst OP, Lodowski DT, Elstner M, Hegemann P, Brown LS, Kandori H (2014) Microbial and animal rhodopsins: structures, functions, and molecular mechanisms. Chem Rev 114:126–163

Farrens DL, Altenbach C, Yang K, Hubbell WL, Khorana HG (1996) Requirement of rigid-body motion of transmembrane helices for light activation of rhodopsin. Science 274:768–770

Geiser AH, Sievert MK, Guo LW, Grant JE, Krebs MP, Fotiadis D, Engel A, Ruoho AE (2006) Bacteriorhodopsin chimeras containing the third cytoplasmic loop of bovine rhodopsin activate transducin for GTP/GDP exchange. Protein Sci 15:1679–1690

Govorunova EG, Spudich EN, Lane CE, Sineshchekov OA, Spudich JL (2011) New channelrhodopsin with a red-shifted spectrum and rapid kinetics from *Mesostigma viride*. MBio 2:e00115–e00111

Govorunova EG, Sineshchekov OA, Janz R, Liu X, Spudich JL (2015) Natural light-gated anion channels: a family of microbial rhodopsins for advanced optogenetics. Science 349:647–650

Govorunova EG, Sineshchekov OA, Li H, Spudich JL (2017) Microbial rhodopsins: diversity, mechanisms, and Optogenetic applications. Annu Rev Biochem 86:845–872

Grote M, Engelhard M, Hegemann P (2014) Of ion pumps, sensors and channels - perspectives on microbial rhodopsins between science and history. Biochim Biophys Acta 1837:533–545

Gushchin I, Shevchenko V, Polovinkin V, Kovalev K, Alekseev A, Round E, Borshchevskiy V, Balandin T, Popov A, Gensch T, Fahlke C, Bamann C, Willbold D, Buldt G, Bamberg E, Gordeliy V (2015) Crystal structure of a light-driven sodium pump. Nat Struct Mol Biol 22:390–395

Hasemi T, Kikukawa T, Kamo N, Demura M (2016) Characterization of a cyanobacterial chloride-pumping rhodopsin and its conversion into a proton pump. J Biol Chem 291:355–362

Havelka WA, Henderson R, Oesterhelt D (1995) Three-dimensional structure of halorhodopsin at 7 Å resolution. J Mol Biol 247:726–738

Hegemann P (2008) Algal sensory photoreceptors. Annu Rev Plant Biol 59:167–189

Hoff WD, Jung KH, Spudich JL (1997) Molecular mechanism of photosignaling by archaeal sensory rhodopsins. Annu Rev Biophys Biomol Struct 26:223–258

Honda N, Tsukamoto T, Sudo Y (2017) Comparative evaluation of the stability of seven-transmembrane microbial rhodopsins to various physicochemical stimuli. Chem Phys Lett 682:6–14

Hosaka T, Yoshizawa S, Nakajima Y, Ohsawa N, Hato M, DeLong EF, Kogure K, Yokoyama S, Kimura-Someya T, Iwasaki W, Shirouzu M (2016) Structural mechanism for light-driven transport by a new type of chloride ion pump, *Nonlabens marinus* rhodopsin-3. J Biol Chem 291:17488–17495

Hou SY, Govorunova EG, Ntefidou M, Lane CE, Spudich EN, Sineshchekov OA, Spudich JL (2012) Diversity of *Chlamydomonas* channelrhodopsins. Photochem Photobiol 88: 119–128

Huang PS, Boyken SE, Baker D (2016) The coming of age of de novo protein design. Nature 537:320–327

Imamoto Y, Shichida Y, Hirayama J, Tomioka H, Kamo N, Yoshizawa S (1992) Nanosecond laser photolysis of phoborhodopsin: from *Natronobacterium pharaonis* appearance of KL and L intermediates in the photocycle at room temperature. Photochem Photobiol 56: 1129–1134

Inoue K, Ono H, Abe-Yoshizumi R, Yoshizawa S, Ito H, Kogure K, Kandori H (2013a) A light-driven sodium ion pump in marine bacteria. Nat Commun 4:1678

Inoue K, Tsukamoto T, Sudo Y (2013b) Molecular and evolutionary aspects of microbial sensory rhodopsins. Biochim Biophys Acta 1837:562–577

Inoue K, Kato Y, Kandori H (2014a) Light-driven ion-translocating rhodopsins in marine bacteria. Trends Microbiol 23:91–98

Inoue K, Koua FH, Kato Y, Abe-Yoshizumi R, Kandori H (2014b) Spectroscopic study of a light-driven chloride ion pump from marine bacteria. J Phys Chem B 118:11190–11199

Inoue K, Tsukamoto T, Shimono K, Suzuki Y, Miyauchi S, Hayashi S, Kandori H, Sudo Y (2015) Converting a light-driven proton pump into a light-gated proton channel. J Am Chem Soc 137:3291–3299

Inoue K, Ito S, Kato Y, Nomura Y, Shibata M, Uchihashi T, Tsunoda SP, Kandori H (2016a) A natural light-driven inward proton pump. Nat Commun 7:13415

Inoue K, Nomura Y, Kandori H (2016b) Asymmetric functional conversion of eubacterial light-driven ion pumps. J Biol Chem 291:9883–9893

Irieda H, Morita T, Maki K, Homma M, Aiba H, Sudo Y (2012) Photoinduced regulation of the chromatic adaptive gene expression by anabaena sensory rhodopsin. J Biol Chem 287:32485–32493

Ito S, Kato HE, Taniguchi R, Iwata T, Nureki O, Kandori H (2014) Water-containing hydrogen-bonding network in the active center of channelrhodopsin. J Am Chem Soc 136:3475–3482

Jung KH, Trivedi VD, Spudich JL (2003) Demonstration of a sensory rhodopsin in eubacteria. Mol Microbiol 47:1513–1522

Kanehara K, Yoshizawa S, Tsukamoto T, Sudo Y (2017) A phylogenetically distinctive and extremely heat stable light-driven proton pump from the eubacterium *Rubrobacter xylanophilus* DSM 9941T. Sci Rep 7:44427

Katayama K, Sekharan S, Sudo Y (2015) Color tuning in retinylidene proteins. In: Yawo H, Kandori H, Koizumi A (eds) Optogenetics: light-sensing proteins and their applications. Springer Japan, Tokyo, 89–107

Kato HE, Zhang F, Yizhar O, Ramakrishnan C, Nishizawa T, Hirata K, Ito J, Aita Y, Tsukazaki T, Hayashi S, Hegemann P, Maturana AD, Ishitani R, Deisseroth K, Nureki O (2012) Crystal structure of the channelrhodopsin light-gated cation channel. Nature 482:369–374

Kato HE, Inoue K, Abe-Yoshizumi R, Kato Y, Ono H, Konno M, Ishizuka T, Hoque MR, Hososhima S, Kunitomo H, Ito J, Yoshizawa S, Yamashita K, Takemoto M, Nishizawa T, Taniguchi RK, Maturana AD, Iino Y, Yawo H, Ishitani R, Kandori H, Nureki O (2015a) Structural basis for Na^+ transport mechanism by a light-driven Na^+ pump. Nature 521:48–53

Kato HE, Kamiya M, Sugo S, Ito J, Taniguchi R, Orito A, Hirata K, Inutsuka A, Yamanaka A, Maturana AD, Ishitani R, Sudo Y, Hayashi S, Nureki O (2015b) Atomistic design of microbial opsin-based blue-shifted optogenetics tools. Nat Commun 6:7177

Kitajima-Ihara T, Furutani Y, Suzuki D, Ihara K, Kandori H, Homma M, Sudo Y (2008) Salinibacter sensory rhodopsin: sensory rhodopsin I-like protein from a eubacterium. J Biol Chem 283:23533–23541

Klare JP, Bordignon E, Engelhard M, Steinhoff HJ (2004) Sensory rhodopsin II and bacteriorhodopsin: light activated helix F movement. Photochem Photobiol Sci 3:543–547

Konno M, Kato Y, Kato HE, Inoue K, Nureki O, Kandori H (2016) Mutant of a light-driven sodium ion pump can transport cesium ions. J Phys Chem Lett 7:51–55

Kouyama T, Kanada S, Takeguchi Y, Narusawa A, Murakami M, Ihara K (2010) Crystal structure of the light-driven chloride pump halorhodopsin from *Natronomonas pharaonis*. J Mol Biol 396: 564–579

Koyanagi M, Terakita A (2008) Gq-coupled rhodopsin subfamily composed of invertebrate visual pigment and melanopsin. Photochem Photobiol 84:1024–1030

Kurihara M, Sudo Y (2015) Microbial rhodopsins: wide distribution, rich diversity and great potential. Biophys Physicobiol 12:121–129

Lanyi JK (2004) Bacteriorhodopsin. Annu Rev Physiol 66:665–688

Lin JY, Knutsen PM, Muller A, Kleinfeld D, Tsien RY (2013) ReaChR: a red-shifted variant of channelrhodopsin enables deep transcranial optogenetic excitation. Nat Neurosci 16:1499–1508

Lórenz-Fonfría VA, Resler T, Krause N, Nack M, Gossing M, Fischer von Mollard G, Bamann C, Bamberg E, Schlesinger R, Heberle J (2013) Transient protonation changes in channelrhodopsin-2 and their relevance to channel gating. Proc Natl Acad Sci USA 110: E1273–E1281

Lórenz-Fonfría VA, Muders V, Schlesinger R, Heberle J (2014) Changes in the hydrogen-bonding strength of internal water molecules and cysteine residues in the conductive state of channelrhodopsin-1. J Chem Phys 141:22D507

Luck M, Mathes T, Bruun S, Fudim R, Hagedorn R, Tran Nguyen TM, Kateriya S, Kennis JT, Hildebrandt P, Hegemann P (2012) A photochromic histidine kinase rhodopsin (HKR1) that is bimodally switched by ultraviolet and blue light. J Biol Chem 287:40083–40090

Luecke H, Schobert B, Richter HT, Cartailler JP, Lanyi JK (1999) Structure of bacteriorhodopsin at 1.55 Å resolution. J Mol Biol 291:899–911

Marti T, Rosselet SJ, Otto H, Heyn MP, Khorana HG (1991) The retinylidene Schiff base counterion in bacteriorhodopsin. J Biol Chem 266:18674–18683

Matsuno-Yagi A, Mukohata Y (1977) Two possible roles of bacteriorhodopsin; a comparative study of strains of *Halobacterium halobium* differing in pigmentation. Biochem Biophys Res Commun 78:237–243

Miranda MR, Choi AR, Shi L, Bezerra AG Jr, Jung KH, Brown LS (2009) The photocycle and proton translocation pathway in a cyanobacterial ion-pumping rhodopsin. Biophys J 96:1471–1481

Mogi T, Stern LJ, Marti T, Chao BH, Khorana HG (1988) Aspartic acid substitutions affect proton translocation by bacteriorhodopsin. Proc Natl Acad Sci USA 85:4148–4152

Moukhametzianov R, Klare JP, Efremov R, Baeken C, Goppner A, Labahn J, Engelhard M, Buldt G, Gordeliy VI (2006) Development of the signal in sensory rhodopsin and its transfer to the cognate transducer. Nature 440:115–119

Muders V, Kerruth S, Lorenz-Fonfria VA, Bamann C, Heberle J, Schlesinger R (2014) Resonance Raman and FTIR spectroscopic characterization of the closed and open states of channelrhodopsin-1. FEBS Lett 588:2301–2306

Muroda K, Nakashima K, Shibata M, Demura M, Kandori H (2012) Protein-bound water as the determinant of asymmetric functional conversion between light-driven proton and chloride pumps. Biochemistry 51:4677–4684

Nagel G, Ollig D, Fuhrmann M, Kateriya S, Musti AM, Bamberg E, Hegemann P (2002) Channelrhodopsin-1: a light-gated proton channel in green algae. Science 296:2395–2398

Nagel G, Szellas T, Huhn W, Kateriya S, Adeishvili N, Berthold P, Ollig D, Hegemann P, Bamberg E (2003) Channelrhodopsin-2, a directly light-gated cation-selective membrane channel. Proc Natl Acad Sci USA 100:13940–13945

Nakatsuma A, Yamashita T, Sasaki K, Kawanabe A, Inoue K, Furutani Y, Shichida Y, Kandori H (2011) Chimeric microbial rhodopsins containing the third cytoplasmic loop of bovine rhodopsin. Biophys J 100:1874–1882

Niho A, Yoshizawa S, Tsukamoto T, Kurihara M, Tahara S, Nakajima Y, Mizuno M, Kuramochi H, Tahara T, Mizutani Y, Sudo Y (2017) Demonstration of a light-driven SO_4^{2-} transporter and its spectroscopic characteristics. J Am Chem Soc 139(12):4376–4389

Oesterhelt D, Stoeckenius W (1971) Rhodopsin-like protein from the purple membrane of *Halobacterium halobium*. Nat New Biol 233: 149–152

Oesterhelt D, Stoeckenius W (1973) Functions of a new photoreceptor membrane. Proc Natl Acad Sci USA 70:2853–2857

Ogren JI, Mamaev S, Russano D, Li H, Spudich JL, Rothschild KJ (2014) Retinal chromophore structure and Schiff base interactions in red-shifted channelrhodopsin-1 from *Chlamydomonas augustae*. Biochemistry 53:3961–3970

Oka T, Yagi N, Fujisawa T, Kamikubo H, Tokunaga F, Kataoka M (2000) Time-resolved x-ray diffraction reveals multiple conformations in the M-N transition of the bacteriorhodopsin photocycle. Proc Natl Acad Sci USA 97:14278–14282

Olson KD, Zhang XN, Spudich JL (1995) Residue replacements of buried aspartyl and related residues in sensory rhodopsin I: D201N produces inverted phototaxis signals. Proc Natl Acad Sci USA 92: 3185–3189

Prigge M, Schneider F, Tsunoda SP, Shilyansky C, Wietek J, Deisseroth K, Hegemann P (2012) Color-tuned channelrhodopsins for multiwavelength optogenetics. J Biol Chem 287:31804–31812

Racker E, Stoeckenius W (1974) Reconstitution of purple membrane vesicles catalyzing light-driven proton uptake and adenosine triphosphate formation. J Biol Chem 249:662–663

Radu I, Bamann C, Nack M, Nagel G, Bamberg E, Heberle J (2009) Conformational changes of channelrhodopsin-2. J Am Chem Soc 131:7313–7319

Ritter E, Stehfest K, Berndt A, Hegemann P, Bartl FJ (2008) Monitoring light-induced structural changes of Channelrhodopsin-2 by UV-visible and Fourier transform infrared spectroscopy. J Biol Chem 283:35033–35041

Sasaki J, Brown LS, Chon YS, Kandori H, Maeda A, Needleman R, Lanyi JK (1995) Conversion of bacteriorhodopsin into a chloride ion pump. Science 269:73–75

Sasaki J, Spudich JL (1999) Proton circulation during the photocycle of sensory rhodopsin II. Biophys J 77:2145–2152

Sasaki K, Yamashita T, Yoshida K, Inoue K, Shichida Y, Kandori H (2014) Chimeric proton-pumping rhodopsins containing the cytoplasmic loop of bovine rhodopsin. PLoS One 9:e91323

Schneider F, Grimm C, Hegemann P (2015) Biophysics of channelrhodopsin. Annu Rev Biophys 44:167–186

Schobert B, Lanyi JK (1982) Halorhodopsin is a light-driven chloride pump. J Biol Chem 257:10306–10313

Shibata M, Yamashita H, Uchihashi T, Kandori H, Ando T (2010) High-speed atomic force microscopy shows dynamic molecular processes in photoactivated bacteriorhodopsin. Nat Nanotechnol 5:208–212

Shichida Y, Imai H (1998) Visual pigment: G-protein-coupled receptor for light signals. Cell Mol Life Sci 54:1299–1315

Shimono K, Ikeura Y, Sudo Y, Iwamoto M, Kamo N (2001) Environment around the chromophore in pharaonis phoborhodopsin: mutation analysis of the retinal binding site. Biochim Biophys Acta 1515: 92–100

Shimono K, Hayashi T, Ikeura Y, Sudo Y, Iwamoto M, Kamo N (2003) Importance of the broad regional interaction for spectral tuning in Natronobacterium pharaonis phoborhodopsin (sensory rhodopsin II). J Biol Chem 278:23882–23889

Sineshchekov OA, Jung KH, Spudich JL (2002) Two rhodopsins mediate phototaxis to low- and high-intensity light in Chlamydomonas Reinhardtii. Proc Natl Acad Sci USA 99:8689–8694

Sineshchekov OA, Sasaki J, Phillips BJ, Spudich JL (2008) A Schiff base connectivity switch in sensory rhodopsin signaling. Proc Natl Acad Sci USA 105:16159–16164

Slotboom DJ (2014) Structural and mechanistic insights into prokaryotic energy-coupling factor transporters. Nat Rev Microbiol 12:79–87

Spudich JL, Bogomolni RA (1984) Mechanism of colour discrimination by a bacterial sensory rhodopsin. Nature 312:509–513

Spudich JL, Jung K-H (2005) Microbial rhodopsin: phylogenetic and functional diversity .Handbook of photosensory receptors. Wiley-VCH Verlag GmbH & Co. KGaA, Weinheim

Subramaniam S, Gerstein M, Oesterhelt D, Henderson R (1993) Electron diffraction analysis of structural changes in the photocycle of bacteriorhodopsin. EMBO J 12:1–8

Sudo Y, Spudich JL (2006) Three strategically placed hydrogen-bonding residues convert a proton pump into a sensory receptor. Proc Natl Acad Sci USA 103:16129–16134

Sudo Y, Iwamoto M, Shimono K, Kamo N (2001a) Pharaonis phoborhodopsin binds to its cognate truncated transducer even in the presence of a detergent with a 1:1 stoichiometry. Photochem Photobiol 74:489–494

Sudo Y, Iwamoto M, Shimono K, Sumi M, Kamo N (2001b) Photoinduced proton transport of pharaonis phoborhodopsin (sensory rhodopsin II) is ceased by association with the transducer. Biophys J 80: 916–922

Sudo Y, Furutani Y, Wada A, Ito M, Kamo N, Kandori H (2005a) Steric constraint in the primary photoproduct of an archaeal rhodopsin from regiospecific perturbation of C-D stretching vibration of the retinyl chromophore. J Am Chem Soc 127:16036–16037

Sudo Y, Okuda H, Yamabi M, Fukuzaki Y, Mishima M, Kamo N, Kojima C (2005b) Linker region of a halobacterial transducer protein interacts directly with its sensor retinal protein. Biochemistry 44:6144–6152

Sudo Y, Yamabi M, Kato S, Hasegawa C, Iwamoto M, Shimono K, Kamo N (2006) Importance of specific hydrogen bonds of archaeal rhodopsins for the binding to the transducer protein. J Mol Biol 357: 1274–1282

Sudo Y, Furutani Y, Spudich JL, Kandori H (2007) Early photocycle structural changes in a bacteriorhodopsin mutant engineered to transmit photosensory signals. J Biol Chem 282:15550–15558

Sudo Y, Ihara K, Kobayashi S, Suzuki D, Irieda H, Kikukawa T, Kandori H, Homma M (2011a) A microbial rhodopsin with a unique retinal composition shows both sensory rhodopsin II and bacteriorhodopsin-like properties. J Biol Chem 286:5967–5976

Sudo Y, Yuasa Y, Shibata J, Suzuki D, Homma M (2011b) Spectral tuning in sensory rhodopsin I from *Salinibacter ruber*. J Biol Chem 286: 11328–11336

Sudo Y, Okazaki A, Ono H, Yagasaki J, Sugo S, Kamiya M, Reissig L, Inoue K, Ihara K, Kandori H, Takagi S, Hayashi S (2013) A blue-shifted light-driven proton pump for neural silencing. J Biol Chem 288:20624–20632

Suzuki D, Furutani Y, Inoue K, Kikukawa T, Sakai M, Fujii M, Kandori H, Homma M, Sudo Y (2009) Effects of chloride ion binding on the photochemical properties of salinibacter sensory rhodopsin I. J Mol Biol 392:48–62

Suzuki D, Irieda H, Homma M, Kawagishi I, Sudo Y (2010) Phototactic and chemotactic signal transduction by transmembrane receptors and transducers in microorganisms. Sensors (Basel) 10:4010–4039

Swartz TE, Szundi I, Spudich JL, Bogomolni RA (2000) New photointermediates in the two photon signaling pathway of sensory rhodopsin-I. Biochemistry 39:15101–15109

Takahashi T, Mochizuki Y, Kamo N, Kobatake Y (1985) Evidence that the long-lifetime photointermediate of s-rhodopsin is a receptor for negative phototaxis in *Halobacterium halobium*. Biochem Biophys Res Commun 127:99–105

Takahashi T, Yan B, Mazur P, Derguini F, Nakanishi K, Spudich JL (1990) Color regulation in the archaebacterial phototaxis receptor phoborhodopsin (sensory rhodopsin II). Biochemistry 29:8467–8474

Tittor J, Haupts U, Haupts C, Oesterhelt D, Becker A, Bamberg E (1997) Chloride and proton transport in bacteriorhodopsin mutant D85T: different modes of ion translocation in a retinal protein. J Mol Biol 271:405–416

Tsukamoto T, Inoue K, Kandori H, Sudo Y (2013) Thermal and spectroscopic characterization of a proton pumping rhodopsin from an extreme thermophile. J Biol Chem 288:21581–21592

Tsukamoto T, Mizutani K, Hasegawa T, Takahashi M, Honda N, Hashimoto N, Shimono K, Yamashita K, Yamamoto M, Miyauchi S, Takagi S, Hayashi S, Murata T, Sudo Y (2016) X-ray crystallographic structure of Thermophilic Rhodopsin: implications for high thermal stability and optogenetic function. J Biol Chem 291:12223–12232

Váró G (2000) Analogies between halorhodopsin and bacteriorhodopsin. Biochim Biophys Acta 1460:220–229

Váró G, Brown LS, Sasaki J, Kandori H, Maeda A, Needleman R, Lanyi JK (1995a) Light-driven chloride ion transport by halorhodopsin from *Natronobacterium pharaonis*. 1. The photochemical cycle. Biochemistry 34:14490–14499

Váró G, Zimányi L, Fan X, Sun L, Needleman R, Lanyi JK (1995b) Photocycle of halorhodopsin from *Halobacterium salinarium*. Biophys J 68:2062–2072

Váró G, Brown LS, Needleman R, Lanyi JK (1996) Proton transport by halorhodopsin. Biochemistry 35:6604–6611

Wegener AA, Klare JP, Engelhard M, Steinhoff HJ (2001) Structural insights into the early steps of receptor-transducer signal transfer in archaeal phototaxis. EMBO J 20:5312–5319

Wietek J, Wiegert JS, Adeishvili N, Schneider F, Watanabe H, Tsunoda SP, Vogt A, Elstner M, Oertner TG, Hegemann P (2014) Conversion of channelrhodopsin into a light-gated chloride channel. Science 344:409–412

Yagasaki J, Suzuki D, Ihara K, Inoue K, Kikukawa T, Sakai M, Fujii M, Homma M, Kandori H, Sudo Y (2010) Spectroscopic studies of a sensory rhodopsin I homologue from the archaeon Haloarcula vallismortis. Biochemistry 49:1183–1190

Yamashita T, Terakita A, Shichida Y (2000) Distinct roles of the second and third cytoplasmic loops of bovine rhodopsin in G protein activation. J Biol Chem 275:34272–34279

Yan B, Takahashi T, Johnson R, Spudich JL (1991) Identification of signaling states of a sensory receptor by modulation of lifetimes of stimulus-induced conformations: the case of sensory rhodopsin II. Biochemistry 30:10686–10692

Ye S, Zaitseva E, Caltabiano G, Schertler GF, Sakmar TP, Deupi X, Vogel R (2010) Tracking G-protein-coupled receptor activation using genetically encoded infrared probes. Nature 464:1386–1389

Yoshizawa S, Kumagai Y, Kim H, Ogura Y, Hayashi T, Iwasaki W, DeLong EF, Kogure K (2014) Functional characterization of flavobacteria rhodopsins reveals a unique class of light-driven chloride pump in bacteria. Proc Natl Acad Sci USA 111:6732–6737